Journal of Immunological Methods 423 (2015) 99–103

Contents lists available at ScienceDirect

Journal of Immunological Methods

journal homepage: www.elsevier.com/locate/jim

Quantification of apoptosis and necroptosis at the single cell level by a combination of Imaging Flow Cytometry with classical Annexin V/propidium iodide staining

Sabine Pietkiewicz, Jörn H. Schmidt, Inna N. Lavrik *

Department of Translational Inflammation Research, Institute of Experimental Internal Medicine, Otto von Guericke University, Magdeburg, Germany

ARTICLE INFO

Article history:
Received 13 November 2014
Received in revised form 15 April 2015
Accepted 30 April 2015
Available online 11 May 2015

Keywords:
Necroptosis
Apoptosis
Death receptor
Imaging flow cytometry
Annexin V/propidium iodide

ABSTRACT

Precisely identifying the type of programmed cell death is one of the key questions in contemporary biomedical research. We developed a straightforward approach allowing quantitative discrimination between two types of cell death on the single cell level: apoptosis and necroptosis. This method uses the combination of imaging flow cytometry with classical Annexin V/propidium iodide staining, which allows for the ascertainment of typical features of dying cells: exposure of the phospholipid phosphatidylserine and the loss of membrane integrity. Image-based analysis of nuclear morphology enables us to distinguish between secondary necrotic/late apoptotic and necroptotic cells directly in one assay. This is a major advantage compared to other contemporary approaches of necroptosis detection, which require a parallel application of several methods. This approach can be used for the quantitative assessment of cell death in cell and systems biology studies of signal transduction networks.

1. Introduction

Programmed cell death (PCD) is essential for regulation of homeostasis and elimination of unneeded, damaged, or infected cells in multicellular organisms (Galluzzi et al., 2014). PCD deregulation contributes to cancer, as well as neurodegenerative and autoimmune diseases. Apoptosis is one of the best studied forms of programmed cell death which depends on the activation of cysteine-dependent aspartate-specific proteases - caspases (Krammer et al., 2007; Lavrik and Krammer, 2012; Schleich et al., 2012). Apoptosis can be triggered by a number of factors including chemotherapeutic drugs, growth factor withdrawal and death receptor (DR) activation. Recently, major progress has been achieved in the investigation of non-apoptotic forms of cell death, particularly programmed necrosis or necroptosis (Ofengeim and Yuan, 2013; Galluzzi et al., 2011). Necroptosis is crucially dependent on the activation of both kinases RIP1 and RIP3, leading to oligomerization of the pseudokinase MLKL and subsequently plasma membrane rupture (Cho et al., 2011; Moriwaki and Chan, 2013; Vandenabeele et al., 2010; Wang et al., 2014). Specific inhibitors of the necroptotic signaling pathway, necrostatins, were developed to target the kinase activity of RIP1 (Degterev et al., 2005, 2008). However, despite the fascinating progress in understanding necroptotic signaling, a straightforward methodology to distinguish between these two types of cell death is currently missing (Vanden Berghe et al., 2010, 2013; Makarov et al., 2013). A combination of several pharmacological and transgenic methods of PCD analysis is implemented conventionally to distinguish between apoptosis or necroptosis and is mostly associated with a number of technical difficulties (Galluzzi et al., 2014). Here we describe an imaging flow cytometry-based approach allowing for the ultimate quantitative distinction between programmed necrosis and apoptosis at the single cell level.

Cells undergoing apoptosis or necrosis have clearly distinct morphological features. The hallmarks of the apoptotic pathway are phosphatidylserine exposure on the cellular surface occurring at the initial or early apoptosis stages, which is followed by membrane blebbing, nuclear fragmentation, decreased cellular volume and a formation of apoptotic bodies (Krammer et al., 2007). Morphological features of programmed necrosis include early plasma membrane rupture, rapid cytoplasmic and nuclear swelling and organelle breakdown (Vandenabeele et al., 2010). In this work to measure cell death we used the imaging flow cytometer FlowSight® (Amnis®, part of EMD Millipore) for cell death detection. FlowSight® belongs to the cutting edge imaging flow cytometers that provide unique opportunities in detecting and preparing images of individual cells analyzed from the bulk cell population. The combination of microscopy and flow cytometry in one device makes it possible to take images of a bright field and up to 10 fluorescence channels in 20× magnification of several thousand cells in a short period of time. In addition, various image features can be analyzed, providing valuable

Abbreviations: PCD, programmed cell death; DR, death receptor; PI, propidium iodide; RIP, Receptor-interacting serine–threonine kinase; MLKL, mixed lineage kinase domain-like Protein; Nec, necrostatin; CD95L, CD95 ligand; SFL, super fas ligand.

* Corresponding author. Tel.: +49 391 6754767; fax: +49 391 6743006.
E-mail addresses: sabine.pietkiewicz@med.ovgu.de (S. Pietkiewicz), joern.schmidt@med.ovgu.de (J.H. Schmidt), inna.lavrik@med.ovgu.de (I.N. Lavrik).

http://dx.doi.org/10.1016/j.jim.2015.04.025
0022-1759/

information on cellular functions. Hence, this method uses the powerful combination of two techniques: the high-throughput measurement of a large number of cells by flow cytometry and the information on microscopy images including automated analysis. This cutting edge technology in combination with the classical Annexin V/propidium iodide staining allowed us to establish the method for distinguishing apoptosis and necroptosis at the single cell level.

2. Material and methods

2.1. Cell culture and cell death induction

282 Jurkat cells were cultivated at 37 °C and 5% CO_2 in RPMI media (Biochrom) with 10% heat-inactivated FCS (Life Technologies) and 1% penicillin/streptomycin (Merck Millipore). CD95-mediated apoptosis was triggered *via* administration of 100 ng CD95L (SuperFasLigand (SFL), Enzo) for 16 h, while CD95L-mediated necroptosis was induced by 100 ng SFL for 16 h after pre-incubation of pan-caspase inhibitor zVAD-fmk (50 μM) (Bachem) and IAP antagonist BV6 (5 μM) (kindly provided by Genentech, Inc.) for 1 h.

2.2. Annexin V/propidium iodide staining

0.5–1 × 10^6 cells were stimulated to induce cell death. At an appropriate time point, cells were harvested by transferring them with the complete medium into 1.5 ml reaction tubes. Cells were centrifuged at 500 ×*g* for 5 min at 4 °C and the supernatant was aspirated. Cells were washed with 1 ml PBS and resuspended in 100 μl staining buffer (Annexin V-FLUOS staining Kit, Roche) by mixing 2 μl of Annexin-V-FLUOS and 2 μl propidium iodide (PI) in incubation buffer according to manufacturer's instructions. The cells were incubated for 15 min at room temperature and protected from light. After centrifugation at 500 ×*g* for 5 min at 4 °C, the staining buffer was aspirated and cells were resuspended in 100 μl PBS. Samples were not stored, but analyzed immediately.

2.3. Quantification of necroptotic, early and late apoptotic cell populations

Samples were analyzed with the imaging flow cytometer FlowSight® (Amnis®, part of EMD Millipore). The 488 nm laser was used for excitation. Debris and doublets were gated out. Bright field (430–480 nm), Annexin V-FLUOS (505–560 nm) and PI (595–642 nm) channel were measured and at least 10,000 events of single cells per sample were collected. Color compensation is necessary as FLUOS and PI have overlapping emission spectra. Additional single-labeled samples were prepared, which contain dead cells and serve as a positive control for single staining of Annexin V-FLUOS or PI, respectively. Color compensation was used to eliminate false positive FLUOS-fluorescence in the channel in which PI is acquired. For analysis the IDEAS version 6.0 was used. Gating strategy was the following. First, focused single cells are identified (using gradient root mean square of the bright field image then bright field area and aspect ratio, respectively) (Table 1, Suppl. Fig. 1). Depending on fluorescence intensity of Annexin V-FLUOS and PI, the populations can be distinguished into double negative (healthy) cells, Annexin-V positive (early apoptotic cells) and double positive (late apoptotic and necroptotic) cells. Using the image based features intensity threshold (>30%) and contrast morphology for the PI-channel, discrimination between late apoptotic and necroptotic cell of the double positive population is achieved. (Please find a detailed definition of the IDEAS features in Table 1.).

3. Results

3.1. Using Annexin V/propidium iodide staining to identify healthy and dying cells

CD95 is a member of the DR family. Triggering CD95 induces cell death in the sensitive cells. To induce apoptosis Jurkat cells were stimulated with 100 ng CD95L for 16 h. To trigger necroptosis, Jurkat cells stimulated with 100 ng CD95L for 16 h after pre-incubation with 5 μM IAP antagonist BV6 and 50 μM caspase inhibitor zVAD-fmk for 1 h. This was followed by the conventional Annexin V-FLUOS and propidium iodide (PI) staining of the cells and imaging flow cytometry. Annexin V is a protein that binds to the phospholipid phosphatidylserine, but cannot enter the cell. Phosphatidylserine is located at the inner side of the membrane. However, upon apoptosis induction, its normal distribution in the cell is perturbed and it becomes exposed at the outer membrane. This feature is used in Annexin V staining for the detection of early apoptotic cells. The membrane-impermeable dye PI binds directly to the DNA, which is only possible upon membrane damage, occurring at late apoptotic or early necroptotic events. We could clearly monitor major stages of cell death. Non-stimulated cells have a round morphology observed in the bright field channel. In addition, they could be categorized as double negative because neither Annexin V, nor PI staining could be detected (Fig. 1a). Early apoptotic cells lose their round shape and form the first apoptotic "blebs", which can be monitored in the bright field channel (Fig. 1b). Furthermore, Annexin V staining could be detected at this stage, indicating phosphatidylserine exposure. At early apoptotic stage, the membrane remains intact, preventing PI staining; thus, early apoptotic cells can be classified as single positive or Annexin V positive (Fig. 1b). At next stage, if apoptosis had taken place *in vivo*, apoptotic cells would have been phagocytized by macrophages or neighboring cells. However, this does not occur under cell culture conditions (Poon et al., 2014). In the latter case, cells typically undergo so-called secondary necrosis, which is accompanied by outer membrane rupture. Due to the membrane damage, PI can penetrate into the cells and thereby be detected. Thus, these cells are double positive, *e.g.* Annexin V/PI-stained (Figs. 1c, 2a). Notably, upon necroptosis/programmed necrosis induction, cells can be classified as double positive as well, as their plasma membrane is damaged and not only PI, but also Annexin V penetrate

Table 1
| Description of the functions used for image-based analysis of PI-stained nucleus (source: Amnis® Imaging Flow Cytometer).

Feature/mask	Description
Contrast feature	The contrast feature measures the sharpness quality of an image by detecting large changes of pixel values in the image and is useful for the selection of focused objects. For every pixel, the slopes of the pixel intensities are computed using the 3 × 3 block around the pixel.
Morphology mask	The morphology mask includes all pixels within the outermost image contour. This mask, which is used in fluorescence images, is highly recommended for use in calculating the values of overall shape-based features.
Intensity feature	The intensity feature is the sum of the background subtracted pixel values within the masked area of the image.
Threshold mask	The threshold mask is used to exclude pixels, based on a percentage of the range of intensity values as defined by the starting mask. The user chooses the starting mask when creating the threshold mask.
Gradient RMS	The gradient root mean square (RMS) feature measures the sharpness quality of an image by detecting large changes of pixel values in the image and is useful for the selection of focused objects. The gradient RMS feature is computed using the average gradient of a pixel normalized for variations in intensity levels.
Area	The number of microns squared in a mask is equal to the area. The number of pixels is converted to μm^2. Note that 1 pixel = 1 μm^2.
Aspect ratio	Aspect Ratio is the value of Minor Axis divided by the one of the Major Axis and describes how round or oblong an object is.

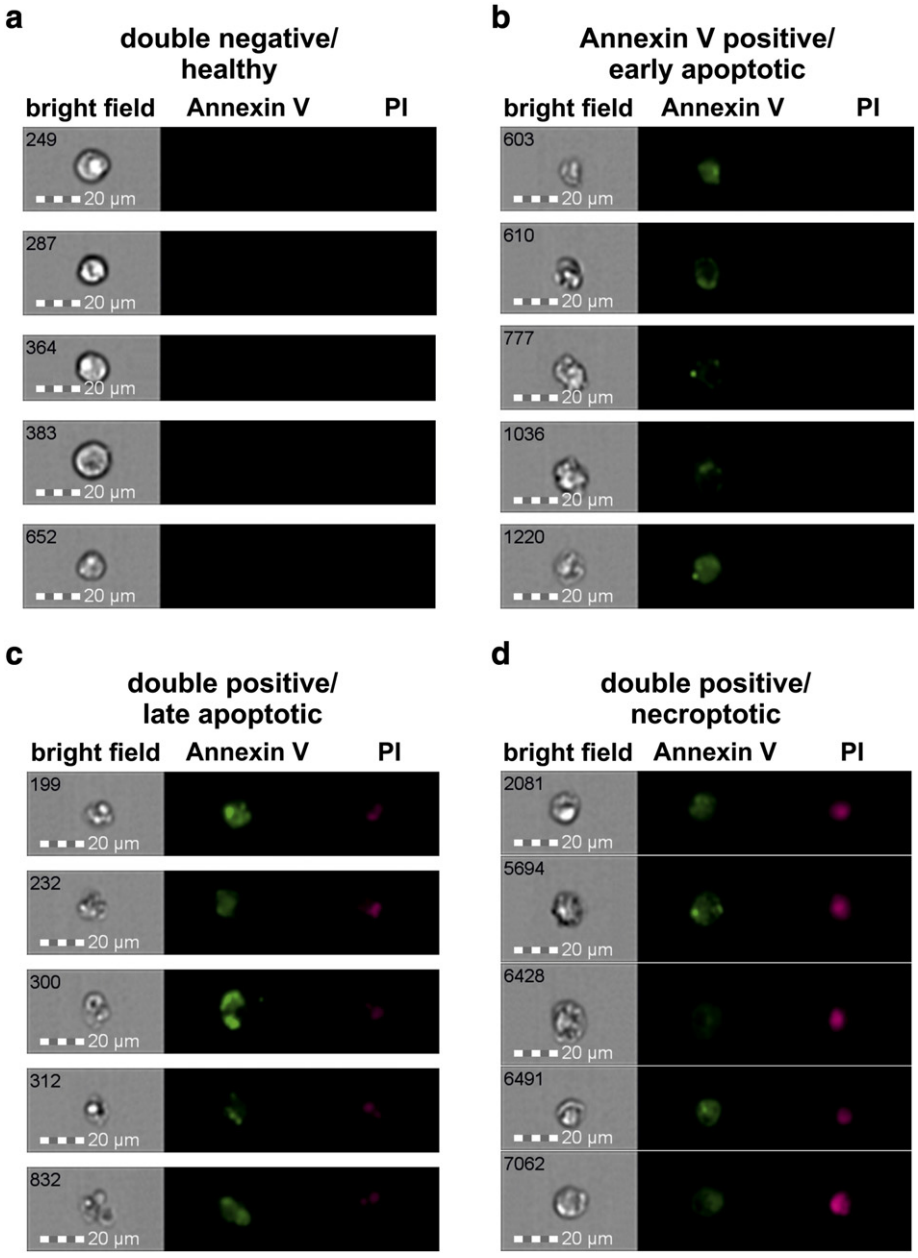

Fig. 1. Representative pictures of cells undergoing apoptosis and necroptosis. (a) Double negative healthy cells, (b) Annexin V positive early apoptotic cells, (c) double positive late apoptotic cells and (d) double positive necroptotic cells, like identified in Fig. 2, are shown. PI = propidium iodide. To trigger apoptosis Jurkat cells were stimulated with 100 ng CD95 Ligand (CD95L) for 16 h. To trigger necroptosis Jurkat cells stimulated with 100 ng CD95L for 16 h after pre-incubation with 5 µM IAP antagonist BV6 and 50 µM caspase inhibitor zVAD-fmk for 1 h. The representative images for four populations are shown. Annexin V and PI staining and analysis with FlowSight® (Amnis®, part of EMD Millipore) were then performed as described.

inside the cell, the latter of which binds to phosphatidylserine from the inner side of the membrane (Figs. 1d, 2a). Noteworthy, it is not possible to distinguish between secondary necrotic/late apoptotic and necrotic cells in this double positive population using classical flow cytometry.

3.2. Image based analysis of PI-stained nuclei to discriminate late apoptotic and necroptotic cells

To distinguish between apoptotic and necroptotic cells in our approach, we use differences in their morphology. Importantly, Annexin V/PI-stained double positive late apoptotic cells are different from double positive necroptotic cells (Fig. 1c, d). Indeed, the late apoptotic cells are shrunken, characterized by Annexin V positive apoptotic blebs and spots with high intensity of PI staining, reflecting condensed chromatin at the later apoptotic stages (Figs. 1c, 2a). In the case of necroptotic cells, the PI staining is more diffuse and thereby an even more intense fluorescence signal is detected (Figs. 1d, 2a). We found special parameters that allow for distinguishing between these two populations (Fig. 2a, Table 1). Using the feature “contrast morphology” of the analysis software IDEAS (Table 1), we have derived a quantitative parameter that characterizes the difference between diffuse staining of the swollen necroptotic nuclei and the sharpness of the condensed apoptotic nuclei. The feature “intensity threshold” of IDEAS Software (Table 1) gave rise to the second parameter that is based on the difference in fluorescence intensity of the PI-signal between apoptotic and necroptotic cells. Indeed, apoptotic nuclei have only small areas of high PI-intensity due to chromatin condensation, while the swollen necroptotic nuclei show bright PI staining all over the nuclear area. Applying these two parameters to a dot plot diagram of the double positive

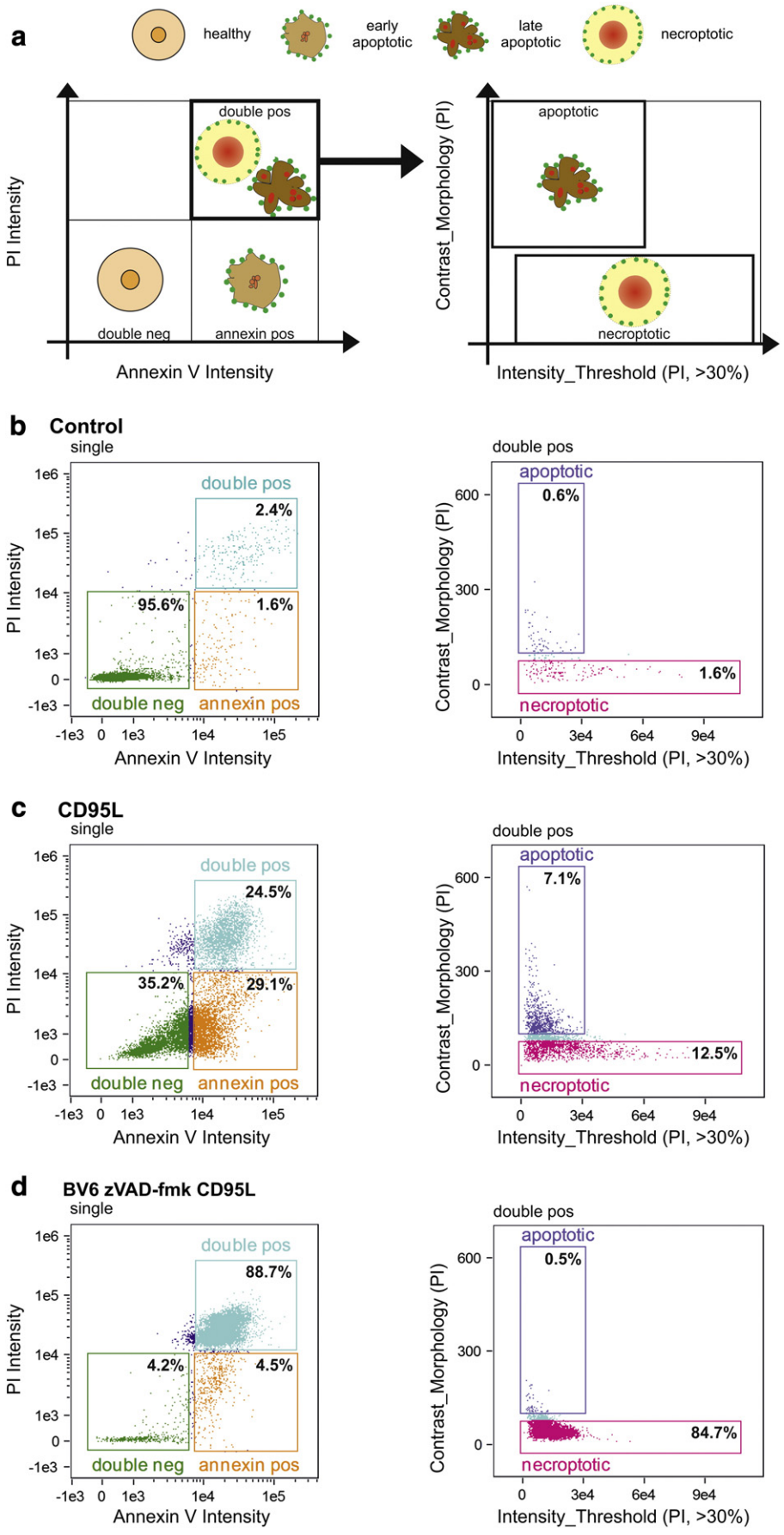
a
healthy
early apoptotic
late apoptotic
necroptotic
double pos
double neg
annexin pos
PI Intensity
Annexin V Intensity
apoptotic
necroptotic
Contrast_Morphology (PI)
Intensity_Threshold (PI, >30%)
b Control
single
2.4%
95.6%
1.6%
0.6%
1.6%
c CD95L
24.5%
35.2%
29.1%
7.1%
12.5%
d BV6 zVAD-fmk CD95L
88.7%
4.2%
4.5%
0.5%
84.7%

population, the late apoptotic cells appear in a distinct population with high "contrast morphology" and low "intensity threshold", while the necroptotic cells are found with low "contrast morphology" and high "intensity threshold" (Fig. 2). Collectively, using these two parameters we could clearly distinguish between late apoptotic and necroptotic populations and quantitatively determine the degree of apoptosis or necroptosis.

The healthy, necroptotic, early and late apoptotic cell populations can be distinguished easily with the presented method. While the untreated sample mostly contains double negative healthy cells (Fig. 2b), the CD95L-treatment induces a high amount of early apoptotic and late apoptotic cells (Fig. 2c). Image based analysis of the double positive population corresponding to the late apoptotic cells reveals a 1:1 ratio of late apoptotic to necrotic cells. In contrast, the stimulation of cells with CD95L in the presence of the pan-caspase inhibitor zVAD-fmk and IAP antagonist BV6 leads to a clear necroptotic switch, as most of the cells appear in the double positive necroptotic population (Fig. 2d).

4. Discussion

This approach provides a major advance compared to comprehensive approaches of cell death detection, as the latter require a combination of several methods in order to ultimately determine the type of cell death (Galluzzi et al., 2014). Necroptotic cell death has to be analyzed indirectly by combining morphological and biochemical assays in time-consuming kinetics and/or under pharmacological or genetic inhibition of key apoptotic and necroptotic players such as the caspase-inhibitors zVAD-fmk, QVD-oph, the RIPK1-inhibitors Nec-1, Nec-1 s or the genetic knockout of Caspase-8, FADD, RIPK3 and MLKL. Hence, the proof of necroptotic cell death can be quite challenging and can hardly be performed quantitatively (Makarov et al., 2013). Determination of the morphological features of cell death by microscopy is an important tool to discriminate apoptotic and necroptotic cells, but very subjective and time-consuming when done in a quantitative manner (Makarov et al., 2013). Our method analyzes biochemical and morphological features of dying cells directly in one measurement by combining classical flow cytometry and microscopy, thereby allowing for the quantification of several thousand cells in a short period of time, together with an objective analysis of pictures by image-based features (George et al., 2004). Additionally, this method includes a simple staining procedure, obtaining rapid and reproducible results.

Supplementary data to this article can be found online at http://dx.doi.org/10.1016/j.jim.2015.04.025.

Competing interest statement

The authors declare no competing financial interests.

Acknowledgments

BV6 was kindly provided by Genentech, Inc. We thank Dr. Kira Bettermann for helpful comments on the manuscript and Stephanie Perniciaro for reading the manuscript. We thank Claudia Arndt for excellent technical assistance. We acknowledge the Ministry of Sciences and Economic Affairs of Saxony-Anhalt (Research Centre Dynamic Systems: Biosystems Engineering, MW-21LMS 5), BMBF (eBIO project "ImmunoQuant" – TPU – 0316170 and, eBIO project "AML" 031A304), DFG (LA 2386/6-1), RFFI 14-04-00699 and Russian Science Foundation 14-44-00011 for supporting our work.

References

Cho, Y., Challa, S., Chan, F.K., 2011. A RNA interference screen identifies RIP3 as an essential inducer of TNF-induced programmed necrosis. Adv. Exp. Med. Biol. 691, 589.
Degterev, A., Huang, Z., Boyce, M., Li, Y., Jagtap, P., Mizushima, N., Cuny, G.D., Mitchison, T.J., Moskowitz, M.A., Yuan, J., 2005. Chemical inhibitor of nonapoptotic cell death with therapeutic potential for ischemic brain injury. Nat. Chem. Biol. 1, 112.
Degterev, A., Hitomi, J., Germscheid, M., Ch'en, I.L., Korkina, O., Teng, X., Abbott, D., Cuny, G.D., Yuan, C., Wagner, G., Hedrick, S.M., Gerber, S.A., Lugovskoy, A., Yuan, J., 2008. Identification of RIP1 kinase as a specific cellular target of necrostatins. Nat. Chem. Biol. 4, 313.
Galluzzi, L., Vanden Berghe, T., Vanlangenakker, N., Buettner, S., Eisenberg, T., Vandenabeele, P., Madeo, F., Kroemer, G., 2011. Programmed necrosis from molecules to health and disease. Int. Rev. Cell Mol. Biol. 289, 1.
Galluzzi, L., Bravo-San Pedro, J.M., Vitale, I., Aaronson, S.A., Abrams, J.M., Adam, D., Alnemri, E.S., Altucci, L., Andrews, D., Annicchiarico-Petruzzelli, M., Baehrecke, E.H., Bazan, N.G., Bertrand, M.J., Bianchi, K., Blagosklonny, M.V., Blomgren, K., Borner, C., Bredesen, D.E., Brenner, C., Campanella, M., Candi, E., Cecconi, F., Chan, F.K., Chandel, N.S., Cheng, E.H., Chipuk, J.E., Cidlowski, J.A., Ciechanover, A., Dawson, T.M., Dawson, V.L., De, L.V., De, M.R., Debatin, K.M., Di, D.N., Dixit, V.M., Dynlacht, B.D., El-Deiry, W.S., Fimia, G.M., Flavell, R.A., Fulda, S., Garrido, C., Gougeon, M.L., Green, D.R., Gronemeyer, H., Hajnoczky, G., Hardwick, J.M., Hengartner, M.O., Ichijo, H., Joseph, B., Jost, P.J., Kaufmann, T., Kepp, O., Klionsky, D.J., Knight, R.A., Kumar, S., Lemasters, J.J., Levine, B., Linkermann, A., Lipton, S.A., Lockshin, R.A., Lopez-Otin, C., Lugli, E., Madeo, F., Malorni, W., Marine, J.C., Martin, S.J., Martinou, J.C., Medema, J.P., Meier, P., Melino, S., Mizushima, N., Moll, U., Munoz-Pinedo, C., Nunez, G., Oberst, A., Panaretakis, T., Penninger, J.M., Peter, M.E., Piacentini, M., Pinton, P., Prehn, J.H., Puthalakath, H., Rabinovich, G.A., Ravichandran, K.S., Rizzuto, R., Rodrigues, C.M., Rubinsztein, D.C., Rudel, T., Shi, Y., Simon, H.U., Stockwell, B.R., Szabadkai, G., Tait, S.W., Tang, H.L., Tavernarakis, N., Tsujimoto, Y., Vanden Berghe, T., Vandenabeele, P., Villunger, A., Wagner, E.F., Walczak, H., White, E., Wood, W.G., Yuan, J., Zakeri, Z., Zhivotovsky, B., Melino, G., Kroemer, G., 2015. Essential versus accessory aspects of cell death: recommendations of the NCCD 2015. Cell Death Differ. 22 (1), 58–73.
George, T.C., Basiji, D.A., Hall, B.E., Lynch, D.H., Ortyn, W.E., Perry, D.J., Seo, M.J., Zimmerman, C.A., Morrissey, P.J., 2004. Distinguishing modes of cell death using the ImageStream multispectral imaging flow cytometer. Cytometry A 59, 237.
Krammer, P.H., Arnold, R., Lavrik, I.N., 2007. Life and death in peripheral T cells. Nat. Rev. Immunol. 7, 532.
Lavrik, I.N., Krammer, P.H., 2012. Regulation of CD95/Fas signaling at the DISC. Cell Death Differ. 19, 36.
Makarov, R., Geserick, P., Feoktistova, M., Leverkus, M., 2013. Cell death in the skin: how to study its quality and quantity? Methods Mol. Biol. 961, 201.
Moriwaki, K., Chan, F.K., 2013. RIP3: a molecular switch for necrosis and inflammation. Genes Dev. 27, 1640.
Ofengeim, D., Yuan, J., 2013. Regulation of RIP1 kinase signalling at the crossroads of inflammation and cell death. Nat. Rev. Mol. Cell Biol. 14, 727.
Poon, I.K., Lucas, C.D., Rossi, A.G., Ravichandran, K.S., 2014. Apoptotic cell clearance: basic biology and therapeutic potential. Nat. Rev. Immunol. 14, 166.
Schleich, K., Warnken, U., Fricker, N., Ozturk, S., Richter, P., Kammerer, K., Schnolzer, M., Krammer, P.H., Lavrik, I.N., 2012. Stoichiometry of the CD95 death-inducing signaling complex: experimental and modeling evidence for a death effector domain chain model. Mol. Cell 47, 306.
Vanden Berghe, T., Vanlangenakker, N., Parthoens, E., Deckers, W., Devos, M., Festjens, N., Guerin, C.J., Brunk, U.T., Declercq, W., Vandenabeele, P., 2010. Necroptosis, necrosis and secondary necrosis converge on similar cellular disintegration features. Cell Death Differ. 17, 922.
Vanden Berghe, T., Grootjans, S., Goossens, V., Dondelinger, Y., Krysko, D.V., Takahashi, N., Vandenabeele, P., 2013. Determination of apoptotic and necrotic cell death in vitro and in vivo. Methods 61, 117.
Vandenabeele, P., Galluzzi, L., Vanden Berghe, T., Kroemer, G., 2010. Molecular mechanisms of necroptosis: an ordered cellular explosion. Nat. Rev. Mol. Cell Biol. 11, 700.
Wang, H., Sun, L., Su, L., Rizo, J., Liu, L., Wang, L.F., Wang, F.S., Wang, X., 2014. Mixed lineage kinase domain-like protein MLKL causes necrotic membrane disruption upon phosphorylation by RIP3. Mol. Cell 54, 133.

Fig. 2. Gating strategy for distinguishing apoptosis and necroptosis and anticipated results for Jurkat cells. (a) Schematic illustration showing the gating strategy of the assay. In the first step, the fluorescence intensity of Annexin V-FLUOS and PI are used to identify healthy (double negative), early apoptotic (Annexin V positive), late apoptotic (double positive) and necroptotic (double positive) cell populations. In the second step, the image-based analysis of sharpness and intensity of the PI staining allow us to distinguish between the late apoptotic and necroptotic populations. Differences in cell size, shape and nuclear morphology of healthy, apoptotic or necroptotic cells are shown in the scheme. The green and magenta dots represent Annexin V-FLUOS and propidium iodide staining, respectively. Jurkat cells were stimulated with 100 ng CD95 Ligand (CD95L) for 16 h, stained with Annexin V/propidium iodide and imaged on FlowSight®. The combination of (b–d, left) Annexin V/PI staining and (b–d, right) image analysis of the nucleus of double positive stained cells allows separation of healthy, necroptotic, early and late apoptotic cell populations. Jurkat cells were (b) left untreated, (c) stimulated with 100 ng CD95L for 16 h or (d) stimulated with 100 ng CD95L for 16 h after pre-incubation with 5 μM IAP antagonist BV6 and 50 μM caspase inhibitor zVAD-fmk for 1 h. neg = negative, pos = positive, PI = propidium iodide. The diagrams show one representative data set out of three independent experiments.